

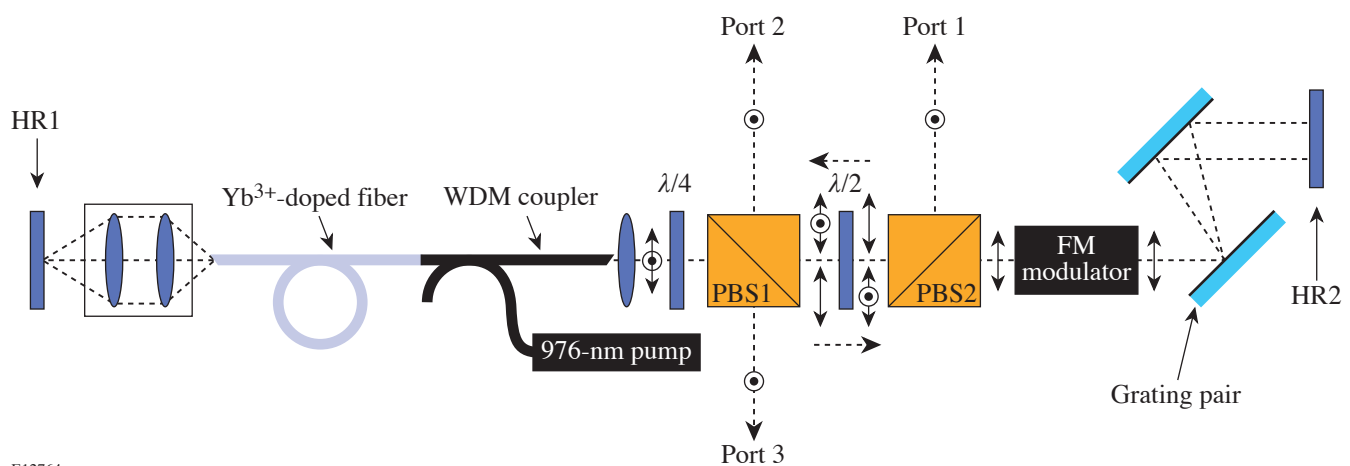
A Tunable, High-Repetition-Rate, Harmonically Mode-Locked, Ytterbium Fiber Laser

Fiber laser and amplifier development in the wavelength region near 1 μm has experienced significant progress owing to the exceptional efficiency and gain bandwidth of ytterbium-doped fibers.^{1–5} In fact, both ytterbium fiber lasers and amplifiers are becoming more attractive than their bulk counterparts due to their confined spatial mode, impressive bandwidth, good pump absorption, ease of alignment, and inherent compatibility with optical fiber. To date, however, experimental efforts regarding ytterbium fiber lasers have been directed only toward fundamental mode-locking, which typically limits pulse repetition rates below 100 MHz.^{1–5}

This article focuses on another important parameter of mode-locked lasers that has thus far attracted little attention in this wavelength regime—high repetition rate. High-repetition-rate ytterbium fiber lasers would be a useful source of ultrafast picket-fence pulse trains that have been proposed to improve the performance of fusion laser systems.⁶ In this scheme, shaped nanosecond pulses are replaced by a train of ultrafast “picket” pulses that deliver the same average power

while increasing the third-harmonic conversion efficiency. A high-repetition-rate and broadly tunable source would also be useful for synchronously pumping multi-GHz optical parametric oscillators.⁷

The laser considered in this research uses a 976-nm pumped linear cavity, shown in Fig. 97.40, similar to that reported by Lefort *et al.* in 2002.² A bulk phase modulator⁸ actively FM mode-locks the laser, enabling synchronization to an external reference frequency. Velocity matching between the optical and microwave fields in the modulator’s LiNbO₃ crystal, in conjunction with a resonant design, offers efficient phase modulation at the device’s resonance frequency ≈ 10.3 GHz. A synthesized microwave signal generator (HP model 83732B) amplified by a traveling-wave tube amplifier (Hughes model 8010H) provides up to 10 W of microwave power to the modulator. To reduce intracavity loss, the crystal facets were antireflection coated, resulting in an insertion loss of $<1\%$ at 1053 nm.



E12764

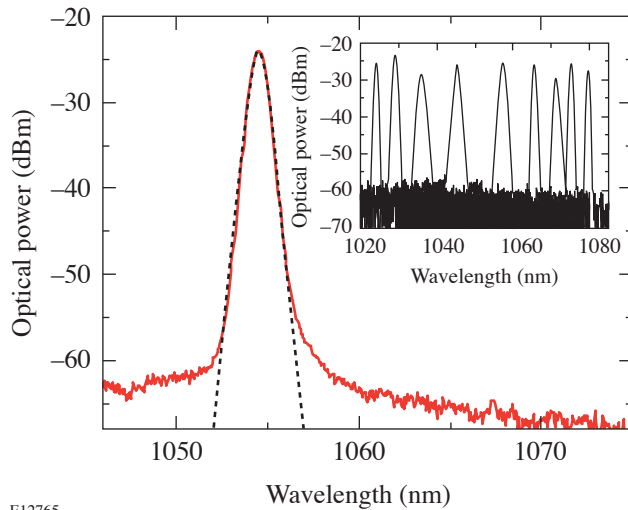
Figure 97.40

Laser cavity configuration: HR, high-reflectivity mirrors; PBS, polarizing beam splitters; WDM, 976/1050-nm wavelength division multiplexer. The double-headed arrows and the dots surrounded by circles represent the horizontal and vertical polarizations, respectively.

The laser delivers output to three different ports, as shown in Fig. 97.40. The combination of a half-wave plate ($\lambda/2$) and a polarizing beam splitter not only provides variable output coupling, yielding up to 38 mW from port 1 and up to 6.5 mW from port 2, but also selects the optimum polarization for the FM modulator and grating pair. Depolarization in the fiber section of the cavity results in 2.5 mW of leakage from port 3.

The mode-locking threshold was measured to be as low as 30 mW, but the pump laser was operated at a power of 150 mW in an effort to maximize the output power and facilitate autocorrelation measurements. All of the results presented in this article were obtained using this pump power and the output from port 1, where the laser had a slope efficiency of 32% (if we consider all three ports the slope efficiency is 40%). The cavity also incorporates a grating pair, which compensates the normal dispersion introduced by 1 m of ytterbium-doped fiber and 1.2 m of fiber associated with the 976/1050 WDM coupler.

A typical mode-locked pulse spectrum, measured with an optical spectrum analyzer (Ando model AQ6315A), reveals a bandwidth of 0.9 nm, as seen in Fig. 97.41. This spectrum is best fit by a sech^2 function shown by the dashed curve. Considering this to be the spectral shape, a 0.9-nm bandwidth (FWHM) implies a 1.3-ps (FWHM) transform-limited sech pulse. According to the simple FM mode-locking theory, an FM modulator in a purely linear dispersionless cavity should



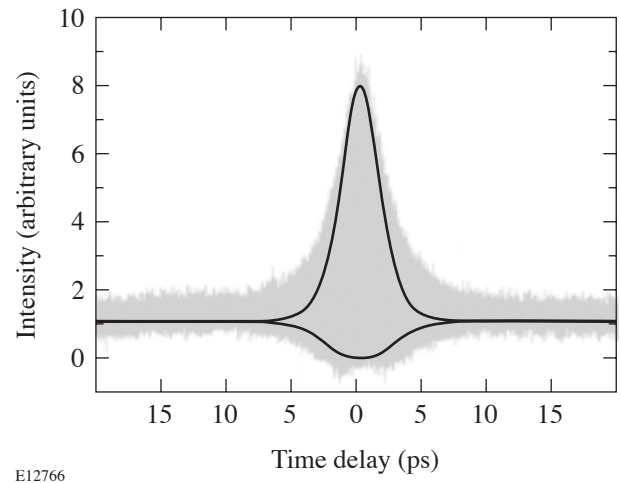
E12765

Figure 97.41

Mode-locked optical pulse spectrum and its associated sech^2 fit. The inset contains superimposed mode-locked spectra illustrating the 1025- to 1080-nm tuning range.

produce chirped Gaussian output pulses with Gaussian spectra.⁹ In light of this, our spectral measurements suggest that cavity dispersion and fiber nonlinearity play a role in shaping the laser pulses.

An interferometric autocorrelator employing two-photon absorption (TPA) in the photocathode of a photomultiplier tube was used to perform autocorrelation measurements (Fig. 97.42).¹⁰ This sensitive diagnostic was required to measure the ≤ 4 -pJ pulses resulting from the extremely high repetition rate. The autocorrelation trace was also best fit by the TPA response to a sech pulse, indicating a pulse width of 2 ps (FWHM).¹¹ Comparing the fit with the 1.3-ps pulse expected for a transform-limited field, the output pulses are found to be broadened by a factor of ≈ 1.5 due to chirp and resulting in a time-bandwidth product of 0.49.



E12766

Figure 97.42

Autocorrelation results. The fit shown in this figure was obtained by using the two-photon absorption response to a 2-ps hyperbolic-secant pulse.

Mode-locked operation was achieved with central wavelengths ranging from 1022 nm to 1080 nm by inserting a razor blade in front of HR2 (not depicted in Fig. 97.40) and adjusting its position. The central wavelength also depended on the driving modulation frequency, the cavity length, and the angular position of mirror HR2. The effect of tuning on the pulse spectrum is shown in the inset of Fig. 97.41, where several different spectra in the tuning range of 1022 to 1080 nm have been superimposed on one another. The spectral shape varies little over the tuning range, although the spectral width increases as the center wavelength is decreased.

Side-mode suppression and timing jitter are two common figures of merit used to evaluate the quality of a mode-locked pulse train. These quantities are derived from the pulse-train power spectrum shown in Fig. 97.43 and obtained using a 25-GHz photodetector with a nominally flat frequency response (New Focus model 1414) and a 26.5-GHz microwave spectrum analyzer (Agilent model E4407B). As expected, the microwave spectrum shown in the inset of Fig. 97.43 is composed of peaks at the 10.31455-GHz driving frequency, its harmonics, and much weaker structures spaced by the 36.8-MHz fundamental repetition rate of the laser cavity (not visible in the figure), which are due to supermode noise.¹² A side-mode suppression of greater than 72 dB was measured with respect to the largest of these side modes. Dividing the laser's mode-locked repetition rate by its fundamental repetition rate reveals that there are 280 pulses simultaneously circulating in this cavity.

Since Fig. 97.43 shows that each peak is δ -function-like, having a FWHM narrower than the minimum resolution (1 Hz)

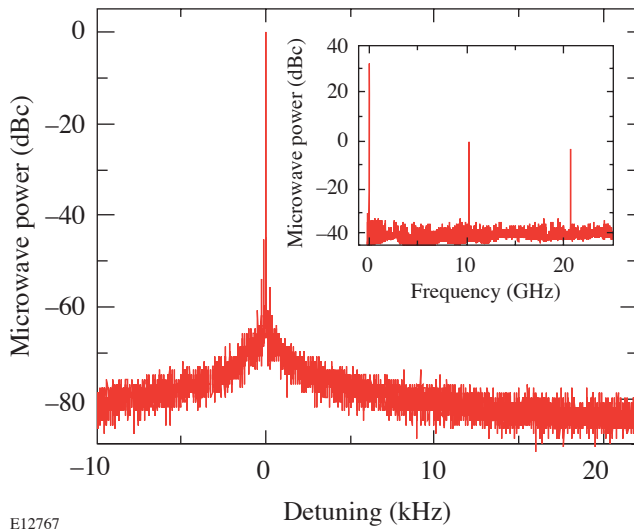


Figure 97.43

The microwave spectrum of the laser versus detuning from the 10.31455-GHz modulation frequency. The figure reveals that the signal at the modulation frequency is located 80 dBs above the noise floor. The inset shows the signal at 0 Hz, the ≈ 10.3 -GHz repetition rate, and the first harmonic located at ≈ 20.6 GHz. Note that the strength of the noise floor has increased (in the inset) due to the reduced resolution of the spectrum analyzer over the broad frequency range used.

of the spectrum analyzer, the timing jitter and pulse energy fluctuations of the output pulse train were characterized. An upper bound on rms timing jitter is related to the integrated spectral power over the offset frequency range f_l - f_h according to¹³

$$\sigma = \frac{1}{2\pi f_m} \left[2 \int_{f_l}^{f_h} L(f) df \right]^{1/2},$$

where σ is the rms timing jitter, f_m is the repetition frequency of the m^{th} harmonic around which this measurement is made, and $L(f)$ is the single-sided phase-noise spectral density detuned from f_m . Integration of the ~ 20 -GHz peak over an offset range from 10 Hz to 12 kHz yields an upper bound on rms timing jitter of 370 fs, which is only slightly larger than the 283-fs jitter measured for the microwave signal generator using the same range. Above 12 kHz, $L(f)$ was dominated by the ≈ -81 -dBc electronic noise floor (seen in Fig. 97.43 at the 20-kHz detuning) of the detector/spectrum analyzer combination, prohibiting an accurate jitter quantization over the typically quoted range (10 Hz to 10 MHz). The rms-energy fluctuations were quantified¹³ over the 10-Hz to 10-MHz range, indicating an rms fluctuation of 16.9 fJ, which corresponds to an energy fluctuation of 0.85% for the 2-pJ pulses.

In conclusion, a tunable, high-repetition-rate, mode-locked, ytterbium fiber laser has been demonstrated. The hyperbolic-secant pulse spectrum indicates that the chirp introduced by the FM modulator is interacting with the cavity dispersion and fiber nonlinearity to play a role in shaping the laser pulses. The pulse-train timing jitter was found to be primarily due to the electronics and could be reduced by using a cleaner signal generator for jitter-sensitive applications. Finally, this laser's output pulse train consisting of linearly polarized, 2-ps chirped pulses could produce up to 38 mW of average power, making it suitable for many future applications.

ACKNOWLEDGMENT

The authors thank Y. Deng for his assistance with the autocorrelation measurements, W. Bittle for his advice on electronics issues, and W. Knox for his support of this work. This work was supported by the U.S. Department of Energy Office of Inertial Confinement Fusion under Cooperative Agreement No. DE-FC03-92SF19460, the University of Rochester, and the New York State Energy Research and Development Authority. The support of DOE does not constitute an endorsement by DOE of the views expressed in this article.

REFERENCES

1. V. Cautaerts *et al.*, Opt. Lett. **22**, 316 (1997).
2. L. Lefort *et al.*, Opt. Lett. **27**, 291 (2002).
3. H. Lim, F. Ö. Ilday, and F. W. Wise, Opt. Lett. **28**, 660 (2003).
4. O. G. Okhotnikov *et al.*, Opt. Lett. **28**, 1522 (2003).
5. A. Liem *et al.*, Appl. Phys. B **71**, 889 (2000).
6. J. E. Rothenberg, Appl. Opt. **39**, 6931 (2000).
7. S. Lecomte *et al.*, Opt. Lett. **27**, 1714 (2002).
8. J. D. Zuegel and D. W. Jacobs-Perkins, "An Efficient, High-Frequency Bulk Phase Modulator," to be published in Applied Optics.
9. D. Kuizenga and A. Siegman, IEEE J. Quantum Electron. **6**, 694 (1970).
10. J. M. Roth, T. E. Murphy, and C. Xu, Opt. Lett. **27**, 2076 (2002).
11. K. Mogi, K. Naganuma, and H. Yamada, Jpn. J. Appl. Phys. 1, Regul. Pap. Short Notes Rev. Pap. **27**, 2078 (1988).
12. F. Rana *et al.*, J. Opt. Soc. Am. B **19**, 2609 (2002).
13. D. von der Linde, Appl. Phys. B **39**, 201 (1986).